

Targeting the T-type calcium channel Cav3.2 in GABAergic arcuate nucleus neurons to treat obesity



Bing Feng¹, Jerney Harms¹, Nirali Patel², Hui Ye², Pei Luo², Valeria Torres Irizarry², Jacob Vidrine¹, Ann Coulter¹, Candida J. Rebello¹, Sangho Yu¹, Jia Fan³, Hans-Rudolf Berthoud¹, Frank Greenway¹, Heike Münzberg¹, Christopher Morrison¹, Pingwen Xu^{2,*}, Yanlin He^{1,*,*,4}

ABSTRACT

Objective: Cav3.2, a T-type low voltage-activated calcium channel widely expressed throughout the central nervous system, plays a vital role in neuronal excitability and various physiological functions. However, the effects of Cav3.2 on energy homeostasis remain unclear. Here, we examined the role of Cav3.2 expressed by hypothalamic GABAergic neurons in the regulation of food intake and body weight in mice and explored the underlying mechanisms.

Methods: Male congenital Cnana1h (the gene coding for Cav3.2) global knockout (Cav3.2KO) mice and their wild type (WT) littermates were first used for metabolic phenotyping studies. By using the CRISPR-Cas9 technique, Cav3.2 was selectively deleted from GABAergic neurons in the arcuate nucleus of the hypothalamus (ARH) by specifically overexpressing Cas9 protein and Cav3.2-targeting sgRNAs in ARH Vgat (Vgat^{ARH}) neurons. These male mutants (Cav3.2KO-Vgat^{ARH}) were used to determine whether Cav3.2 expressed by Vgat^{ARH} neurons is required for the proper regulation of energy balance. Subsequently, we used an electrophysiological patch-clamp recording in *ex vivo* brain slices to explore the impact of Cav3.2KO on the cellular excitability of Vgat^{ARH} neurons.

Results: Male Cav3.2KO mice had significantly lower food intake than their WT littermate controls when fed with either a normal chow diet (NCD) or a high-fat diet (HFD). This hypophagia phenotype was associated with increased energy expenditure and decreased fat mass, lean mass, and total body weight. Selective deletion of Cav3.2 in Vgat^{ARH} neurons resulted in similar feeding inhibition and lean phenotype without changing energy expenditure. These data provides an intrinsic mechanism to support the previous finding on ARH non-AgRP GABA neurons in regulating diet-induced obesity. Lastly, we found that naringenin extract, a predominant flavanone found in various fruits and herbs and known to act on Cav3.2, decreased the firing activity of Vgat^{ARH} neurons and reduced food intake and body weight. These naringenin-induced inhibitions were fully blocked in Cav3.2KO-Vgat^{ARH} mice.

Conclusion: Our results identified Cav3.2 expressed by Vgat^{ARH} neurons as an essential intrinsic modulator for food intake and energy homeostasis, which is a potential therapeutic target in the treatment of obesity.

© 2021 The Author(s). Published by Elsevier GmbH. This is an open access article under the CC BY-NC-ND license (<http://creativecommons.org/licenses/by-nc-nd/4.0/>).

Keywords Cav3.2; GABA neurons; Feeding; Hypothalamus; Obesity; Naringenin

1. INTRODUCTION

Neuronal functions, including action potential (AP) generation, neurotransmitter release, and synaptic plasticity, are tightly modulated by the cytosolic calcium ion (Ca²⁺), the most common signal transduction element in neurons and excitable cells. Voltage-gated calcium channels (VGCCs) are widely expressed in mammalian neurons and excitable cells. They are subdivided into L-type (Cav1.1,

Cav1.2, Cav1.3, and Cav1.4), P/Q-type (Cav2.1), N-type (Cav2.2), R-type (Cav2.3), and T-type (Cav3.1, Cav3.2, and Cav3.3) [1–4]. T-VGCCs are widely expressed in tissues throughout the body, including the central nervous system (CNS) [2,5–7]. They have been reported to play a vital role in the proper regulation of neuronal firing patterns and burst-firing activity in the CNS, and contribute to various physiological functions, including sleep regulation [8,9], acute itch [10], and pain [11].

¹Pennington Biomedical Research Center, Louisiana State University, 6400 Perkins Rd, Baton Rouge, LA, 70808, USA ²The Division of Endocrinology, Diabetes and Metabolism, Department of Medicine, The University of Illinois at Chicago, Chicago, IL, 60612, USA ³The Department of Biochemistry and Molecular Biology, Department of Biochemistry and Molecular Biology, Tulane University School of Medicine, New Orleans, LA, 70112, USA

⁴ Lead correspondence.

*Corresponding author. 835 S Wolcott Ave, MC 613, Chicago, IL, 60612, USA. Fax: +(312)-413-0437. E-mail: pingwenx@uic.edu (P. Xu).

**Corresponding author. 6400 Perkins Road, Basic Science Building, L2024, Baton Rouge, LA, 70808-4124, USA. Fax: +(225)-763-2525. E-mail: Yanlin.He@pbrcc.edu (Y. He).

Received August 21, 2021 • Revision received October 20, 2021 • Accepted November 2, 2021 • Available online 9 November 2021

<https://doi.org/10.1016/j.molmet.2021.101391>

It is well established that the hypothalamus is an essential brain structure for the regulation of feeding behavior and energy homeostasis [12–15]. One of the vital hypothalamic nuclei engaging in this regulation is the arcuate nucleus of the hypothalamus (ARH). Several lines of studies have suggested that ARH neurons that express an amino acid neural transmitter gamma-aminobutyric acid (GABA) play a vital role in promoting food intake and inhibiting energy expenditure [16–18]. Recent studies revealed that GABA transmission mediates the orexigenic effects of classic agouti-related peptide (AgRP) and other GABAergic neurons in the ARH [16,18,19]. Activation of GABAergic, agouti-related protein (AgRP), or non-AgRP GABAergic neurons in the ARH leads to hyperphagia and obesity. In contrast, inhibition of GABA+, but not AgRP neurons in the ARH reduces aging-related weight gain and alleviates leptin deficiency-induced obesity [16]. Together, modulation of ARH GABAergic neuron activity is a fundamental mechanism for body weight regulation. There is a potential to prevent obesity by inhibiting ARH GABAergic neurons. Most of the previous studies focused on the effects of Cav3.2 on neuronal firing activity control in the regulation of anxiety [20], memory [20], chronic pain [11], and epilepsy [21–23]. However, the role of Cav3.2 in feeding behavior and energy homeostasis is still not well understood. Here, we first used a germline loss-of-function mouse model to examine the effects of Cav3.2 on feeding behavior and energy balance in a normal chow diet (NCD) or high-fat diet (HFD) fed condition. Mice with Cav3.2 selectively deleted from vesicular GABA transporter (Vgat)-expressing ARH neurons (Vgat^{ARH}) were used to examine the roles of Cav3.2 expressed by ARH GABA + neurons in energy homeostasis. We explored the potential Cav3.2-dependent mechanisms in the beneficial metabolic effects mediated by the supplementation of naringenin, a predominant flavanone in a variety of fruits and herbs. Our studies provide compelling evidence to support targeting Cav3.2 expressed by ARH GABA + neurons in the treatment of obesity and related metabolic diseases.

2. METHODS

2.1. Mice

Several genetically modified mouse models were used in the current study. *Cana1h*^{-/-} (Cav3.2KO) mice (Jackson Laboratory, #013770) were maintained on a C57BL/6J background. Both WT and *Cana1h*^{-/-} littermates were generated from heterozygous *Cana1h*^{+/-} breeders. We also bred Vgat-ires-Cre mice (Jackson Laboratory, #028862) with Rosa26-EGFP-L10 mice (Jackson Laboratory, #024750) to generate Vgat-ires-Cre/Rosa26-EGFP-L10 mice. Lastly, we breed *Cana1h*^{-/-} mice with Vgat-ires-Cre/Rosa26-EGFP-L10 mice to generate Vgat-ires-Cre/Rosa26-EGFP-L10/Cacna1h^{-/-} mice.

Care of all animals and procedures were approved by Pennington Biomedical Research Center (PBRC) and The University of Illinois at Chicago Institutional Animal Care and Use Committees. Mice were housed in a temperature-controlled environment at 22–24 °C, using a 12-h light and 12-h dark cycle. Unless otherwise stated, the mice were fed with a standard normal chow diet (Cat#5001, LabDiet), and water was provided ad libitum unless otherwise indicated.

2.2. Characterization of feeding behavior and energy homeostasis

Cav3.2KO mice and their control littermates were weaned at three weeks of age on a standard chow diet (5.0% fat, #5001, LabDiet) and singly housed afterward. Some mice were switched to an HFD (60% fat, #D12492, Research Diets) at six weeks of age. Body weight and food intake were measured every four days. Body composition was

determined using quantitative magnetic resonance (QMR). At the end of monitoring, the mice were deeply anesthetized with inhaled isoflurane and sacrificed. The gonadal white adipose tissue (gWAT), the inguinal white adipose tissue (iWAT), and the interscapular brown adipose tissue (BAT) were isolated and weighed.

To characterize the food intake and energy expenditure, we generated another male cohort (Cav3.2KO mice and their control littermates at 12 weeks of age). They were acclimated into the Promethion system (Sable, NV, USA). Mice were housed individually at room temperature (22 °C) under an alternating 12:12-h light–dark cycle. After adaptation for three days, O₂ consumption, CO₂ production, and energy expenditure were monitored when mice were fed ad libitum with NCD. The body composition was measured before and after the mice entered the Promethion system. The energy expenditure was corrected per lean body mass.

2.3. CRISPR-Cas9 deletion of Cav3.2 in the ARH GABA + neurons

AAV vectors carrying sgRNAs targeting mouse *Cacna1h* were designed and constructed by Vector Builder (Chicago, IL). Exon 6 and exon 11 were chosen to be targeted by CRISPR-Cas9. A total of 21 sgRNAs were designed, with seven targeting exon 6 and fourteen targeting exon 11. These sgRNAs were selected using the CRISPR tool (<https://www.sanger.ac.uk/htgt/wge/>) with minimal potential off-target effects. To generate sgRNA expression plasmids, oligonucleotides containing gRNA sequence were created and cloned into the final rAAV backbone with mCherry reporter by Gateway recombination. All 21 sgRNAs were screened for on–target activity using electrophysiology. We used the pCS(puro)-positive plasmid, which expressed a proven positive-sgRNA, as the positive control. The sgRNA#1 (CTGGGCATGTTCCGGCCCTGT) and sgRNA#2 (CTGTTCCGGCCAGAAATGCTAC) were selected to target exon 6 and exon 11 of the *Cacna1h* gene, respectively, due to their relatively high on–target activity and low off-target potentials. As a control, scramble RNAs (GTGTAGTTCGACCATTCTGTG) and (GTTTCAGATCACGTTACCGC) was used to replace the sgRNA#1 and sgRNA#2, respectively. U6 promoter-sgRNAs, CAG promoter-DIO-mCherry-bGH polyA cassettes were cloned into the plasmid # VB201223-1293enK vector (<http://www.addgene.org/61591/>) and further verified by full sequencing. The viruses were packaged and produced by the Vector Builder (Chicago, IL).

At 12 weeks of age, male Vgat-ires-Cre mice were anesthetized with isoflurane and received stereotaxic injections of AAV-FLEX-saCas9 mixed with AAV-DIO-Cav3.2 sgRN/mCherry into both sides of the ARH (Cav3.2KO-Vgat^{ARH}; 250 nL/site, –1.7 mm posterior, ±0.25 mm lateral and –5.8 mm ventral to the Bregma, based on Franklin & Paxinos Mouse Brain Atlas). Another group of male Vgat-ires-Cre mice at the same age received AAV-FLEX-saCas9 mixed with AAV-DIO-scramble sgRN/mCherry injections into the ARH. One week after the virus injections, mice were singly housed and fed a chow diet for 5 weeks. Body weight and food intake were monitored weekly. Body composition was measured at the end of the chow diet-feeding phase. All mice were then switched to HFD feeding for another 6 weeks. To validate accurate and sufficient infection of AAV vectors, all mice were perfused with 10% formalin. Brain sections were cut at 25 μm (5 series) and subjected to histological validation. Only those mice with mCherry on both sides of the ARH were included in data analyses.

In another experiment, a different cohort of male Cav3.2KO-Vgat^{ARH} and control mice were used to test naringenin's effects on feeding behavior. Two weeks after the virus injection, all mice received naringenin intraperitoneal injection for two days (40 mg/kg body weight/day). Food intake and body weight were measured daily for 7 days.

2.4. Electrophysiological recordings

Male and female Vgat-ires-Cre/Rosa26-EGFP-L10, Vgat-ires-Cre/Rosa26-EGFP-L10/Cacna1h^{-/-}, and AAV-injected Vgat-ires-Cre (12 weeks of age) were used for electrophysiological recordings. Mice were deeply anesthetized with isoflurane and transcardially perfused with a modified ice-cold sucrose-based cutting solution (pH 7.3) containing 10 mM NaCl, 25 mM NaHCO₃, 195 mM sucrose, 5 mM glucose, 2.5 mM KCl, 1.25 mM NaH₂PO₄, 2 mM Na-Pyruvate, 0.5 mM CaCl₂, and 7 mM MgCl₂, bubbled continuously with 95% O₂ and 5% CO₂ [24,25]. The mice were then decapitated, and the entire brain was removed and immediately submerged in the cutting solution. Slices (200 μm) were cut with a Leica VT1000 S microtome vibratome (Leica, Germany). Three brain slices containing the LH, ZI, TN, and ARH were obtained for each animal (Bregma -2.06 mm to -1.46 mm; Interaural 1.74 mm–2.34 mm). The slices were recovered for 1 h at 34 °C and then maintained at room temperature in artificial cerebrospinal fluid (aCSF, pH 7.3) containing (126 mM NaCl, 2.5 mM KCl, 2.4 mM CaCl₂, 1.2 mM NaH₂PO₄, 1.2 mM MgCl₂, 5.0 mM glucose, and 21.4 mM NaHCO₃) saturated with 95% O₂ and 5% CO₂ before recording [15,25]. Slices were transferred to a recording chamber and allowed to equilibrate for at least 10 min before recording. The slices were superfused at 34 °C in oxygenated aCSF at a flow rate of 1.8–2 ml/min. EGFP or mCherry labeled neurons in the ARH and vVMH were visualized using epifluorescence and IR-DIC imaging on an upright microscope (Eclipse FN-1, Nikon) equipped with a movable stage (MP-285, Sutter Instrument). For GABA neurons firing activity recording, the patch pipettes with resistances of 3–5 MΩ were filled with intracellular solution (pH 7.3) containing 128 mM K-Gluconate, 10 mM KCl, 10 mM HEPES, 0.1 mM EGTA, 2 mM MgCl₂, 0.05 mM Na-GTP and 0.05 mM Mg-ATP [25]. Recordings were made using a MultiClamp 700B amplifier (Axon Instrument), sampled using Digidata 1440A and analyzed offline with pClamp 10.3 software (Axon Instruments). The firing frequency and membrane potential were recorded under current clamp. For voltage-gated calcium current recording, the pipette solution (pH 7.2) contains 135 mM KMeSO₃, 4 mM NaCl, 10 mM HEPES, 1 mM MgCl₂, 0.5 mM EGTA, 3 mM Mg-ATP, and 0.3 mM Tris-GTP. The voltage-gated calcium currents were evoked by 100-ms pulse delivered every 10 s from -90 mV to -30 mV followed by return to -90 mV holding for 500 ms [26]. Neurons were held at -70 mV between sweeps. Series resistance was monitored during the recording, and the values were generally <10 MΩ and were not compensated. The liquid junction potential was +12.5 mV and was corrected after the experiment. Data were excluded if the series resistance increased dramatically during the experiment or without overshoot for action potential. Currents were amplified, filtered at 1 kHz, and digitized at 20 kHz.

To examine the naringenin's function on GABA neurons, neurons were recorded under the current-clamp mode in response to a puff treatment of different doses of naringenin or vehicle (1% DMSO) [27]. The values for firing rate were averaged within 2-min bin in the presence or absence of naringenin. Neurons that were inhibited (>10% decrease of firing rate) or neurons that were activated (>10% increase of firing rate) in response to naringenin were identified as responsive. Neurons that showed responses less than 10% change of firing rate were identified as non-responsive. To further test whether naringenin regulates calcium currents via the PKA signal pathway, Vgat^{ARH} neurons were pretreated by Rp-cAMP before the naringenin puff treatment.

2.5. Statistical analyses

The data are presented as mean ± SEM (standard error of the mean). Statistical analyses were performed using GraphPad Prism 8.3 to

evaluate normal distribution and variations within and among groups. Methods of statistical analyses were chosen based on the design of each experiment and are indicated in figure legends or main text. $p < 0.05$ was considered to be statistically significant.

2.6. Study approval

Care of all animals and procedures were approved by the PBRC and UIC Institutional Animal Care and Use Committee.

3. RESULTS

3.1. Cav3.2KO mice showed decreased body weight and food intake on a NCD

To examine the physiological roles of Cav3.2 in the regulation of feeding behavior and energy expenditure, we generated a cohort of male and female Cav3.2 deficient *Cacna1h*^{-/-} (Cav3.2KO) mice and their control littermates (Supplemental Fig. 1A). We measured their food intake and body weight after they were weaned at 3 weeks of age. When fed with a NCD, the Cav3.2KO male mice started to show significant body weight difference at around 7 weeks of age compared to their control littermates (Figure 1A). The body weight gain and cumulative food intake were consistently decreased at a similar age (Figure 1B–D). No gender difference was observed in the metabolic effects induced by Cav3.2KO. Female Cav3.2KO also displayed significantly lower body weight and food intake compared to their control littermates (Supplemental Figs. 1B–C). However, we failed to observe any difference in body length of male and female Cav3.2KO mice and their control littermates (Figure 1H and Supplemental Fig. S1D). The body weight difference was due to the loss of both lean and fat mass as indicated by lower lean and fat mass in male Cav3.2KO mice observed at 9 weeks of age (Figure 1E–G).

3.2. Abnormal energy metabolism in Cav3.2KO mice

To determine the mechanisms underlying the lean phenotypes seen in Cav3.2KO mice, another cohort of NCD-fed male Cav3.2KO males and their control littermates (12 weeks of age) were adapted into the Sable Promethion Systems metabolic chambers to measure energy expenditure. Compared to control mice, Cav3.2KO males showed significantly higher energy expenditure primarily during the light cycle when fed ad libitum (Figure 1I–K).

3.3. Cav3.2KO Mice have an attenuated response to HFD

We then characterized body weight phenotypes in male Cav3.2KO mice switched to an HFD at 6 weeks of age. Consistent with our observations in the NCD-fed condition, HFD-fed male Cav3.2KO mice gained significantly less body weight, which was associated with lower HFD intake, compared to their control littermates (Figure 2A–D). In particular, HFD-fed Cav3.2KO males started to have a lower body weight as early as 4 days after HFD feeding, and after 48 days of HFD feeding, Cav3.2KO males gained 6.14 g less body weight than controls (about 15% of control body weight) (Figure 2A–B). This reduced body weight observed in Cav3.2KO males was associated with decreased lean mass, fat mass, and body fluid (Figure 2E–G). Weights of different fat depots, including brown fat (BAT), inguinal white fat (iWAT), and gonadal white fat (gWAT) were significantly lower in Cav3.2 males compared with control littermates (Figure 2H–J). We found that HFD-induced obesogenic expansion with abnormal adipocyte enlargement (hyperplasia) in both iWAT and gWAT depots was largely attenuated in Cav3.2KO males (Figure 2K). In addition, we observed that Cav3.2KO restored BAT morphology with fewer lipid droplets compared to control littermates under HFD

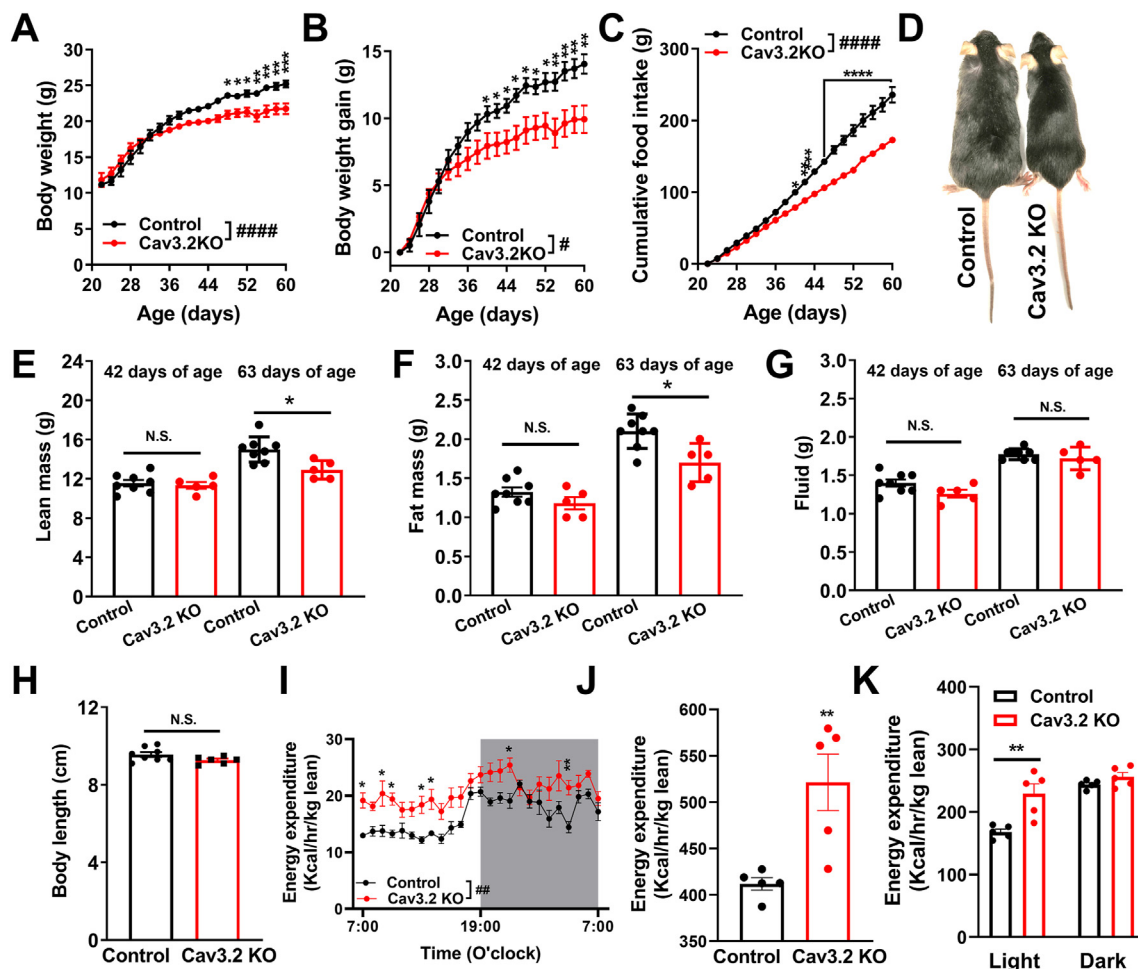


Figure 1: (See also Fig. S1). Cav3.2KO mice showed decreased body weight gain and food intake when fed with chow diet. (A) Body weight, (B) body weight gain, and (C) cumulative food intake of control and Cav3.2KO mice under chow diet feeding ($n = 8$ in control and $n = 6$ in Cav3.2KO groups). (D) Representative image of control and Cav3.2KO mice at age of 8 weeks when fed with chow diet. (E) Lean mass, (F) fat mass, and (G) fluid of control and Cav3.2KO mice ($n = 8$ in control and $n = 6$ in Cav3.2KO groups). (H) Body length of control and Cav3.2KO male mice. (I) 24 h energy expenditure curve, (J) daily energy expenditure, and (K) energy expenditure during light and dark cycle of control and Cav3.2KO mice. ($n = 5$ in control and $n = 5$ in Cav3.2KO groups). Results are presented as mean \pm SEM. *, $P < 0.05$, **, $P < 0.01$, ***, $P < 0.001$, ****, $P < 0.0001$ in two-way ANOVA analysis followed by post hoc Sidak tests. #####, $P < 0.0001$ in unpaired t-tests.

feeding (Figure 2K). Together, our data suggest that the loss of Cav3.2 decreases susceptibility to DIO in male mice.

3.4. Selective knockout of Cav3.2 in Vgat^{ARH} neurons inhibits Vgat^{ARH} neuronal firing activity

The activity dynamics of GABAergic neurons in different hypothalamic regions, including ARH [28,29], lateral hypothalamus (LH) [30,31], tuberal nucleus (TN) [32,33], and zona incerta (ZI) [34,35], plays a vital role in the regulation of feeding behavior, body weight, and energy expenditure. It has been demonstrated that neural excitability is regulated by subtypes of neuronal voltage-activated Ca²⁺ channels, including CAV3.2 [36,37]. CAV3.2 may serve as a critical intrinsic modulator for the neural excitability of hypothalamic GABAergic neurons to control energy homeostasis. To test this hypothesis, we generated both Vgat-ires-Cre/Rosa26-EGFP-L10/Cacna1h^{-/-} (Vgat-Cre/EGFP/Cav3.2KO) mice and control littermates Vgat-ires-Cre/Rosa26-EGFP-L10 mice (Vgat-Cre/EGFP) (Figure 3A). We used the *ex vivo* brain slice whole-cell patch-clamp method to characterize electrophysiological properties of Vgat neurons in the ARH, LH, TN, and ZI (Figure 3B).

Vgat^{ARH} neurons from Vgat-Cre/EGFP/Cav3.2KO mice showed significantly lower firing activity and hyperpolarized resting membrane potential (RMP) compared to the Vgat^{ARH} neurons from control Vgat-Cre/EGFP mice (Figure 3C–E). We also found that total voltage-gated calcium currents were smaller in Cav3.2-deficient Vgat^{ARH} neurons (Figure 3F,G). However, we failed to observe any changes in electrophysiological properties of Cav3.2-deficient Vgat^{LH}, Vgat^{TN}, or Vgat^{ZI} neurons (Supplemental Figs. 2A–I). These data revealed an essential role of Cav3.2 in the activity dynamics of Vgat^{ARH} neurons.

To further test the effects of Cav3.2 expressed by Vgat^{ARH} neurons on food intake and body weight, we used Clustered Regularly Interspaced Short Palindromic Repeats (CRISPR) Cas9 technique to selectively delete Cav3.2 only in the Vgat^{ARH} neurons. We designed and identified two sgRNAs that efficiently induced indel mutations in exon 6 and 11 of the Cacna1h gene (Supplementary Fig. 3A). Both these sgRNAs were constructed into one AAV vector followed by a Cre-dependent FLEX-mCherry sequence (AAV-Cav3.2/sgRNAs-FLEX-mCherry). At 8 weeks of age, male Vgat-ires-Cre mice received stereotaxic injections of a mixture of AAV-Cav3.2/sgRNAs-FLEX-mCherry and AAV-FLEX-saCAS9 (1:1; Cav3.2KO-Vgat^{ARH}) or AAV-scramble-Cav3.2/sgRNAs-FLEX-

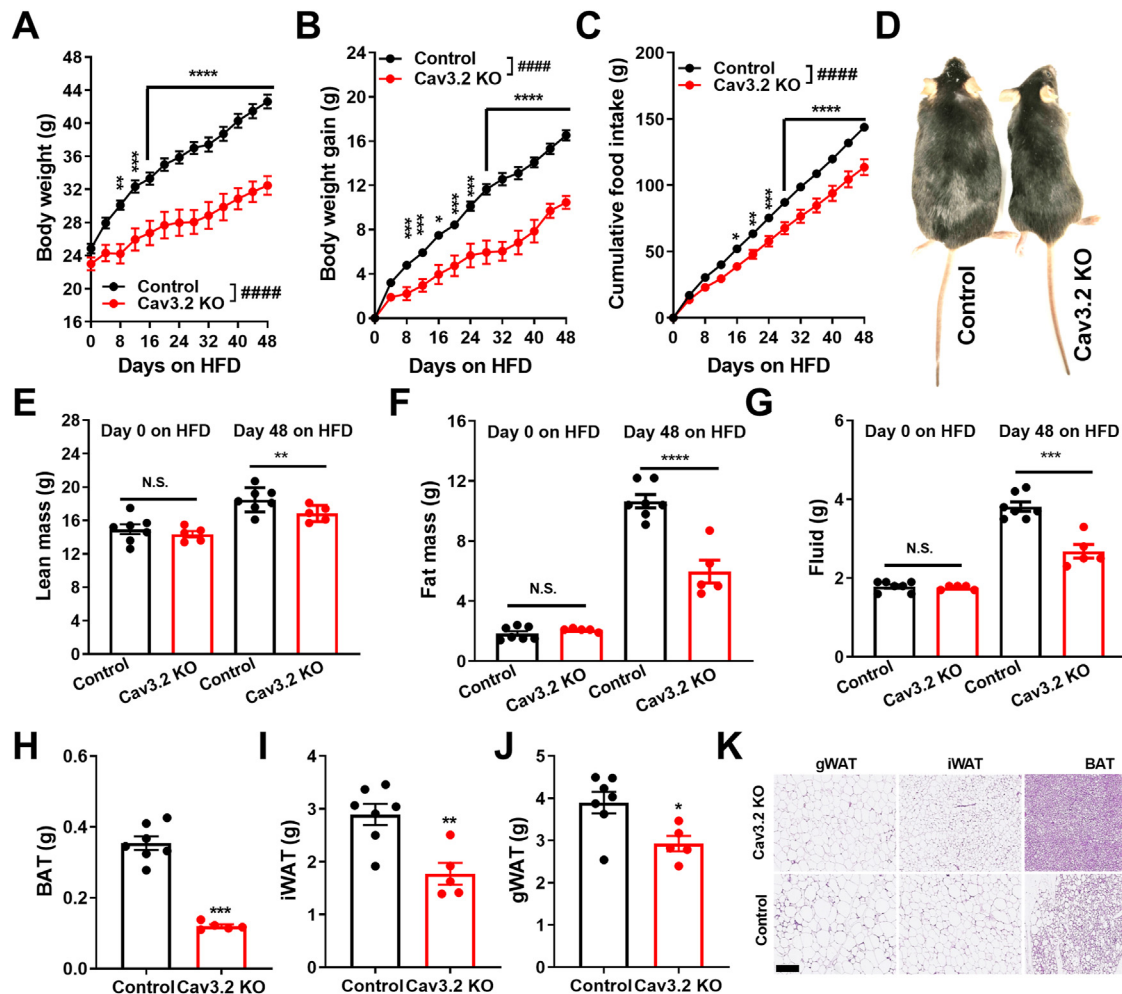


Figure 2: Cav3.2KO mice showed decreased body weight gain and food intake when fed with HFD. (A) Body weight, (B) body weight gain, and (C) cumulative food intake of control and Cav3.2KO mice under HFD feeding ($n = 7$ in control and $n = 5$ in Cav3.2KO groups). (D) Representative image of control and Cav3.2KO mice at age of 8 weeks when fed with HFD. (E) Lean mass, (F) fat mass, and (G) fluid of control and Cav3.2KO mice. (H) BAT, (I) iWAT, and (J) gWAT tissue weight from control and Cav3.2KO mice after 8 weeks of HFD feeding ($n = 7$ in control and $n = 5$ in Cav3.2KO groups). (K) H&E staining of gWAT, iWAT, and BAT tissue. Results are presented as mean \pm SEM. *, $P < 0.05$, **, $P < 0.01$, ***, $P < 0.001$, ****, $P < 0.0001$ in two-way ANOVA analysis followed by post hoc Sidak tests. ####, $P < 0.0001$ in unpaired t-tests.

mCherry and AAV-FLEX-saCAS9 (1:1; control) in both sides of the ARH (Figure 4A). The injection accuracy and infection efficiency were validated by mCherry fluorescence (Figure 4B). We first use the *ex vivo* brain slice patch-clamp method to validate the successful deletion of Cav3.2 in Vgat^{ARH} neurons (Figure 4C). We found that Vgat^{ARH} neurons from male Cav3.2KO-Vgat^{ARH} mice showed lower firing frequency, hyperpolarized RMP, and smaller voltage-gated calcium current when compared to Vgat^{ARH} neurons from control mice (Figure 4D–H). This is consistent with our earlier observations in Vgat-Cre/EGFP/Cav3.2KO mice and validates the Cav3.2KO-Vgat^{ARH} model.

3.5. Selective knockout of Cav3.2 in Vgat^{ARH} neurons reduces food intake and body weight gain

Consistent with the metabolic effects caused by Cav3.2 global KO, selective deletion of Cav3.2 Vgat^{ARH} led to decreased body weight gain and food intake when fed an NCD or an HFD (Figure 5A,B). Cav3.2KO-Vgat^{ARH} mice also showed reduced food intake and feeding efficiency compared to their control littermates when fed with NCD or HFD (Figure 5C–F). The body weight difference on HFD feeding was attributed mainly to decreases in fat mass, more specifically iWAT and

gWAT, but not the other body components (Figure 5G–L). These male Cav3.2KO-Vgat^{ARH} mice showed a similar level of energy expenditure compared to the control mice under NCD feeding before they displayed body weight and lean mass difference (Supplementary Fig. 3A–C), suggesting a hypophagia-induced weight loss. These results demonstrate that Cav3.2 expressed by Vgat^{ARH} neurons is physiologically relevant for the regulation of feeding behavior and subsequent body weight homeostasis.

3.6. Naringenin extract reduces food intake and body weight gain by inhibiting Vgat^{ARH} neurons in a Cav3.2-dependent mechanism

Naringenin, a flavonoid present in sweet oranges and grapefruit, was recently found to improve glucose and lipid homeostasis and mitigate adipose tissue inflammation in rodents and humans [27,38–40]. Naringenin has been shown to interact with voltage-gated ion channels and potentially block VGCCs, including Cav3.2 [41–43]. We speculated that Cav3.2 expressed by Vgat^{ARH} neurons partially mediates the beneficial metabolic effects of naringenin. To test this, we examined the direct electrophysiological effects of naringenin on Vgat^{ARH} neurons and tested whether Cav3.2 is required for these effects. We found that

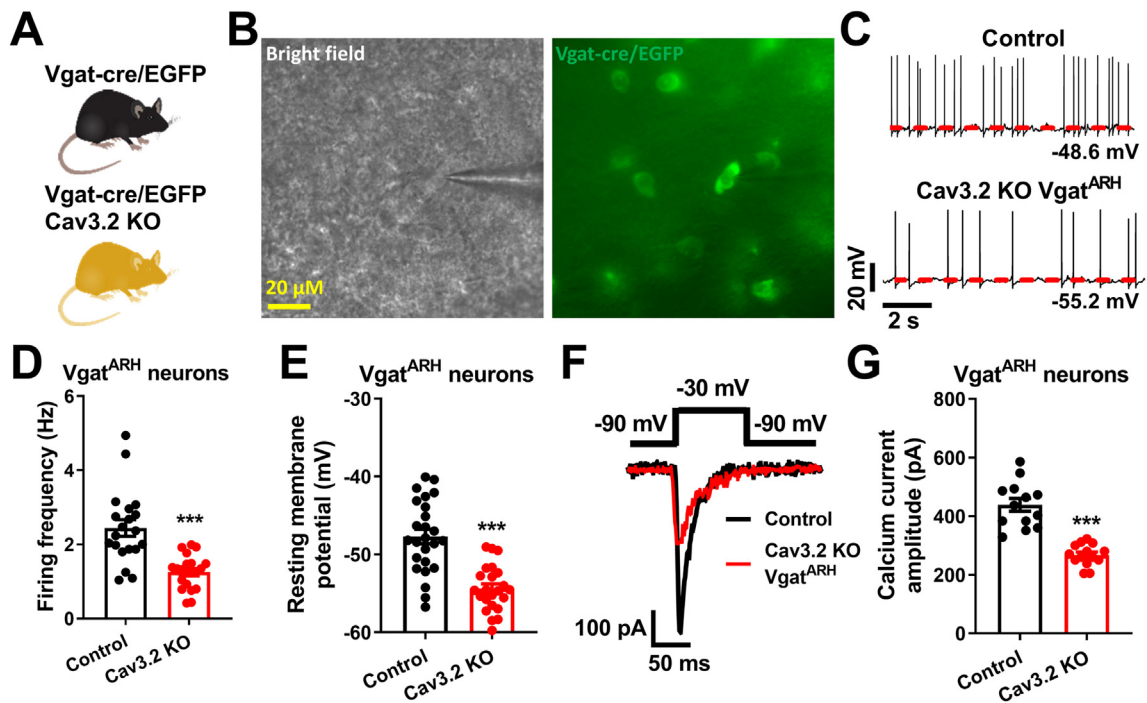


Figure 3: (See also Fig. S2). Vgat^{ARH} neurons firing activity is decreased in Cav3.2KO mice (A) Schematic of Vgat-cre/EGFP and Vgat-cre/EGFP Cav3.2KO mice. (B) Representative images of Vgat-cre/GFP neurons under whole-cell patch clamp recording. Scale bar = 20 μm . (C) Representative spontaneous action potential firing traces and (D) calcium current trace from control and Cav3.2KO Vgat^{ARH} neurons. (E) Summary of action potential firing frequency, (F) resting membrane potential, and (G) calcium current amplitude from control or Cav3.2KO Vgat^{ARH} neurons ($n = 14\text{--}21$ neurons in each group). Results are presented as mean \pm SEM. ***, $P < 0.001$ in two-way ANOVA analysis followed by post hoc Sidak tests.

naringenin dose-dependently inhibited Vgat^{ARH} neurons (Supplementary Fig. 4A–D). 30 μM naringenin was sufficient to block firing activity, reduce RMP, and decrease the voltage-gated calcium current (Figure 6A–E) in control mice. Naringenin stimulated Cl^- secretion in colonic epithelium via a signaling pathway involving the cAMP-dependent protein kinase (PKA) [44]. Native T-type (Cav3.1, Cav3.2, and Cav3.3) channels are differentially regulated by PKA [45–47]. We speculated that Cav3.2 acts through PKA signaling to regulate Vgat^{ARH} neural activity. To directly test this speculation, we pretreated Vgat^{ARH} neurons with 10 μM Rp-cAMP (a membrane-permeable PKA inhibitor) [45] for 10 min and then puff treated Vgat^{ARH} neurons with 30 μM naringenin. The results showed that naringenin failed to decrease firing activity, RMP, and the voltage-gated calcium current in the presence of Rp-cAMP (Supplementary Figure 4 E–G), suggesting a PKA-dependent mechanism. More importantly, the inhibitory effects of naringenin on Vgat^{ARH} neurons were fully blocked in Cav3.2KO-Vgat^{ARH} mice (Figure 6A–B, and F–H), suggesting a Cav3.2-dependent inhibition on Vgat^{ARH} neurons. Together, our results indicate that naringenin inhibits Vgat^{ARH} neurons by regulating the Cav3.2 channel via the PKA signal pathway to reduce voltage-gated calcium current.

Considering the metabolic effects of Cav3.2 and the blood–brain barrier permeability of naringenin [48], we hypothesize that circulating naringenin acts on Cav3.2 expressed by Vgat^{ARH} neurons to regulate energy homeostasis. We found that while two days of naringenin injection (40 mg/kg, once/day, intraperitoneal) significantly decreased food intake and body weight in male control mice, these inhibitory effects of naringenin were blocked in male Cav3.2KO-Vgat^{ARH} mice. Intracerebroventricular (ICV) injection of naringenin (1 μM , 1.5 μl) in DIO mice reduced HFD intake during dark time compared to the vehicle injection (Supplemental Fig. 4E–F). Together, these data

support that Cav3.2 expressed by Vgat^{ARH} neurons is required for the hypophagia and body weight lowering effects of naringenin.

4. DISCUSSION

T-type calcium channels (Cav3.1, Cav3.2, and Cav3.3) play a vital role in the neuronal burst-firing activities in many brain regions [49–51], representing a promising pharmacological target for various diseases or behavioral disorders. However, little is known about the specific functions of these channels in the regulation of energy homeostasis. Here, by using congenital KO mice, we report for the first time that one isoform of T-type calcium channels, Cav3.2, plays an essential role in the regulation of body weight and adiposity by modulating feeding behavior and energy expenditure. Data generated from Cav3.2KO-Vgat^{ARH} mice further demonstrated that the metabolic effects of Cav3.2 are at least partly mediated by modulating spontaneous AP firing and RMP of GABAergic neurons in the ARH. We also provided evidence to support a mediating role of Cav3.2 expressed by Vgat^{ARH} neurons in the beneficial metabolic effects of naringenin, a flavonoid present in citrus fruits, which has been discovered as a potential blocker for T-type calcium channels, including Cav3.2. Together, our data suggest that Cav3.2 expressed by Vgat^{ARH} neurons is a physiological modulator for food intake and energy homeostasis, serving as a prospective therapeutic target in the treatment of obesity.

The best characterized orexigenic neural population in the ARH is the AgRP-expressing neurons. AgRP neurons co-express genes for neuropeptide Y (NPY) [52] and GABA [28] and use AgRP, NPY, and GABA as neurotransmitters to regulate feeding. These neuropeptides play distinct but complementary roles in the regulation of feeding; either GABA or NPY is required for the rapid stimulation of feeding [14]. NPY

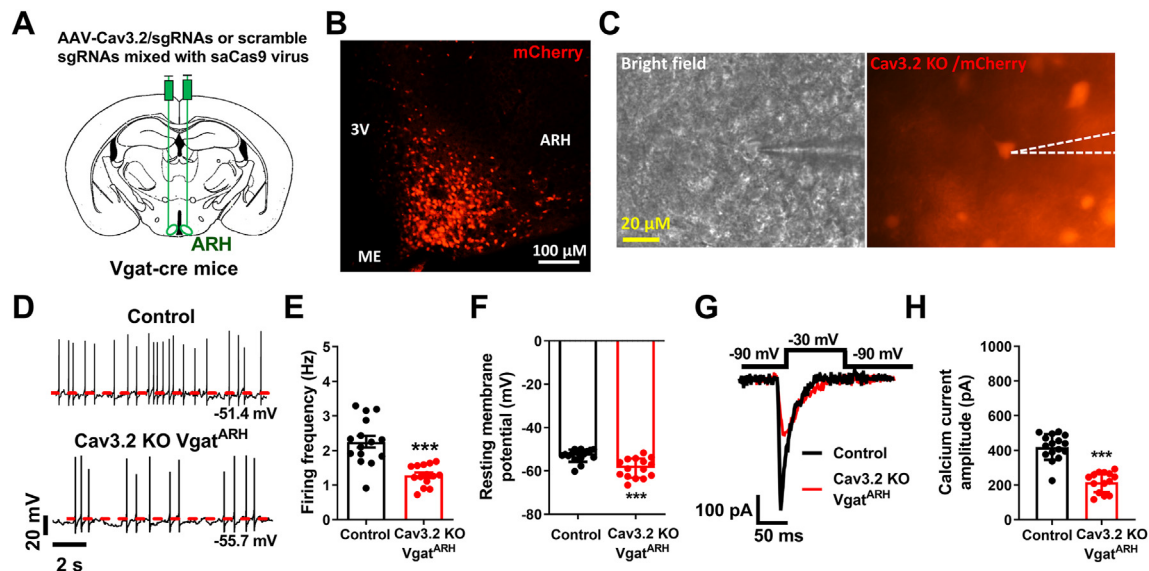


Figure 4: Selectively knockout Cav3.2 from Vgat^{ARH} neurons reduced Vgat^{ARH} neurons firing activity and calcium current. (A) Schematic of experimental strategy to inject AAV-Cav3.2/sgRNA and saCas9 virus in the ARH of Vgat-cre mice. (B) Representative images of Vgat^{ARH} neurons expressed by mCherry. (C) Representative images of Vgat^{ARH} neurons expressed by Cav3.2 sgRNA under whole-cell patch clamp recording. Scale bar = 20 μ m. (D) Representative spontaneous action potential firing traces (E) Summary of action potential firing frequency and (F) resting membrane potential. (G) Calcium current trace from control and Cav3.2KO in Vgat^{ARH} neurons and (H) summary of calcium current amplitude from control or Cav3.2KO Vgat^{ARH} neurons (n = 14–18 neurons in each group). Results are presented as mean \pm SEM. ***, P < 0.001 in two-way ANOVA analysis followed by post hoc Sidak tests.

contributes to maintaining the sustaining hunger selectively on the timescale of a meal [53]. It was recently discovered that AgRP neurons are inhibited within seconds by the sensory detection of food and can drive feeding via a long-lasting hunger signal [54]. This unusual mechanism for controlling behavior is mediated through NPY [53], which extends the duration of AgRP neurons' behavioral effects for tens of minutes beyond the window of their immediate firing. NPY may mediate these sustaining orexigenic effects by acting directly on post-synaptic targets of AgRP neurons to cause durable changes in their activity [55]. Conversely, the neuropeptide AgRP, through action on melanocortin 4 receptor, is sufficient to induce long-lasting potentiation of feeding behavior that persists for days. These prolonged orexigenic effects require several hours to emerge when endogenous AgRP release is stimulated [14,56]. By working together, these neuropeptides contribute to the regulation of temporally distinct phases of eating.

Consistent with the rapid orexigenic effects of GABA released from AgRP neurons, the GABAergic neurons in the ARH potently regulate short-term feeding behavior, as previously reported in the mouse models with neuronal activity acutely manipulated [57–59]. However, the intracellular mechanisms intrinsically modulating ARH GABAergic neurons firing activity and subsequent food intake are unclear. Here we combined Vgat-ires-Cre mice and targeted delivery of AAV vectors carrying Cav3.2 gRNA and Cas9 to selectively knockout Cav3.2 from GABAergic neurons in ARH. Cav3.2KO-Vgat^{ARH} significantly inhibited the firing activity of ARH GABAergic neurons. In line with the regulatory effects of ARH GABAergic neurons on food intake, we also found Cav3.2KO-Vgat^{ARH} mice showed phenotypes of hypophagia and associated body weight loss, suggesting a pivotal role of Cav3.2-Vgat^{ARH} in the regulation of feeding behavior. Although our stereotaxic targeting to the Vgat^{ARH} neurons is precise because of the selective Vgat expression in the ARH structure, we observe a small number of dorsal medial

hypothalamic (DMH) neurons in some animals with a viral infection. We did not observe any differences in food intake and body weight in these animals compared to ARH selectively targeted mice. Thus, we believe that the feeding behavior and body weight changes in these “leaking” mice were mainly attributed to the selective deletion of Cav3.2 in ARH GABAergic neurons. However, a role of Cav3.2 expressed by DMH neurons in body weight regulation cannot be completely ruled out.

Emerging evidence has shown a direct link between the activity of ion channels and systemic energy homeostasis, including central regulation of food intake [15,60–62], energetic balance [63–65], hormone release and response [66–68], as well as the adipocyte cell proliferation [69–72]. Consistently, we found that Cav3.2KO-Vgat^{ARH} resulted in hyperpolarization and hypophagia-induced body weight loss, suggesting an important role of the central Ca²⁺ ion channel in energy balance regulation. It has been extensively reported that intracellular Ca²⁺ appears to be involved in metabolic derangements, including obesity and insulin resistance [73]. Cav3.2KO-Vgat^{ARH} likely modulates the calcium influx to change the firing activity of Vgat^{ARH} neurons and food intake. In supporting this point of view, the RMP and calcium current amplitude were decreased after Cav3.2KO from the Vgat^{ARH} neurons. Acute naringenin treatment hyperpolarized Vgat^{ARH} neurons via inhibition of Cav3.2-mediated calcium currents, however, these data do not entirely exclude the possibility of a calcium influx-independent mechanism mediated by the Cav3.2 ion channel in Vgat^{ARH} neurons.

Two different mouse models were used in this study to investigate the metabolic function of Cav3.2. We found Cav3.2KO dramatically reduced body weight, associated with decreased food intake and increased energy expenditure. CRISPR-mediated Cav3.2KO-Vgat^{ARH} also resulted in decreases in food intake and body weight. However, we failed to observe any changes in energy expenditure of Cav3.2KO-Vgat^{ARH} mice, suggesting a Vgat^{ARH}-independent mechanism.

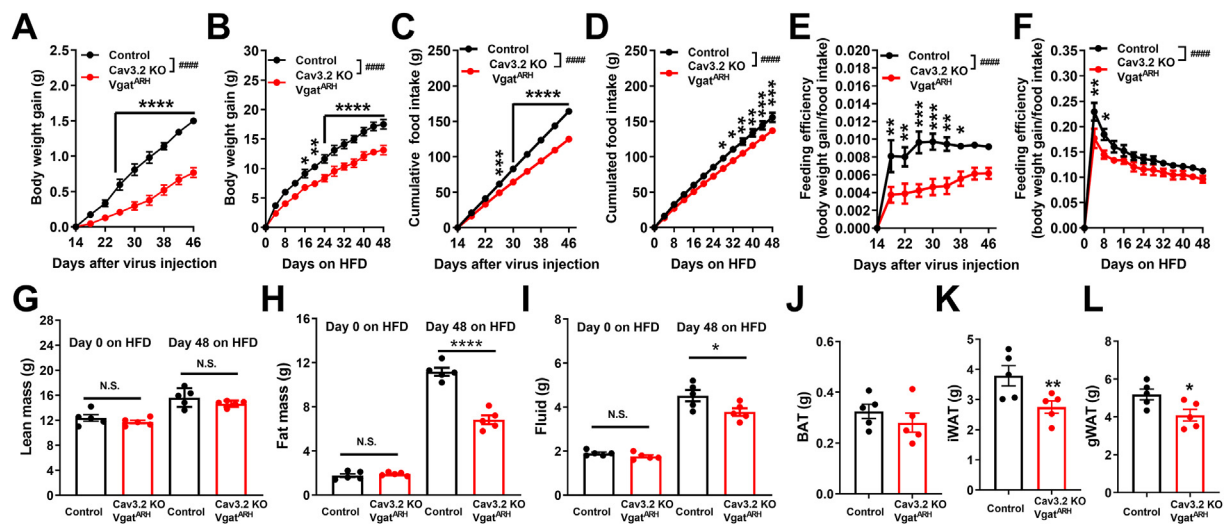


Figure 5: (See also Fig. S3). Knockout Cav3.2 from Vgat^{ARH} neurons reduced animals' food intake and body weight on normal chow diet, and (B) HFD feeding of control and Cav3.2KO Vgat^{ARH} mice. (C) Cumulative food intake on chow diet, and (D) HFD feeding of control and Cav3.2KO Vgat^{ARH} mice. (E) Feeding efficiency on chow diet, and (F) HFD feeding of control and Cav3.2KO Vgat^{ARH} mice. (G) Lean mass, (H) fat mass, and (I) fluid of control and Vgat^{ARH} Cav3.2KO Vgat^{ARH} mice. (J) BAT, (K) iWAT, and (L) gWAT tissue weight from control and Cav3.2KO Vgat^{ARH} mice after 8 weeks of HFD feeding (n = 5 in control and n = 5 in Vgat^{ARH} Cav3.2KO groups). All data are presented as mean ± SEM. *, P < 0.05, **, P < 0.01, ***, P < 0.001, ****, P < 0.0001 in two-way ANOVA analysis followed by post hoc Sidak tests. ####, P < 0.0001 in unpaired t-tests.

Compared to the control mice, the increased energy expenditure induced by Cav3.2KO is mainly in the light phase. This data indicated that Cav3.2 regulates energy expenditure in a circadian-dependent way via some non-Vgat^{ARH} neurons. The gene coding Cav3.2 is strongly expressed in the suprachiasmatic nucleus (SCN) [74,75]. Given that voltage-gated Ca²⁺ currents contribute to the diurnal properties of action potential firing in SCN neurons [76] and that SCN neurons interact with ARH neurons to regulate energy balance [77,78], Cav3.2 expressed by SCN neurons may modulate energy expenditure in a circadian-dependent manner. A further study focusing on the metabolic effects of Cav3.2 in SCN neurons is warranted.

The regulatory effects of Cav3.2 on energy expenditure may also work through peripheral mechanisms. The Cav3.2 encoding gene expresses in cells from many peripheral tissues, including the adipocytes from WAT and BAT [79], myocytes from skeletal muscle [80] and smooth muscle [81], sensory dorsal root ganglion (DRG) neurons, and spinal dorsal horn (SDH) neurons, but not sympathetic neurons [82]. Cav3.2 has been shown to play essential roles in the physiological functions of excitable tissues, i.e., neurons and muscle. For clarification, Cav3.2 expressed by the neurons in the DRG and SDH contributes to inflammatory hyperalgesia and chronic pain [83,84], Cav3.2 expressed by the skeletal muscle contributes to the maintenance of muscle mass and normal function [80], Cav3.2 in the smooth muscle hyperpolarizes and relaxes arteries [85,86].

Conversely, no direct evidence exists to support a physiological function of Cav3.2 expressed by adipocytes. More accurately, the physiological roles of ion channels inside adipose tissue are poorly characterized, due to the fact that adipocytes are non-excitable cells without the ability to generate action potential as neurons or muscles. However, RMP does exist in adipocytes and is maintained by the complement of ion channels. Whereas most biologists would perceive that the RMP is primarily about excitability, the recent data identified a range of critical roles that the RMP has in various cell types beyond the action potential [87]. There is emerging evidence supporting the connection between adipocyte RMP and adipose tissue metabolic

function. In a recent Cell paper [79], Chen et al. have identified a critical K⁺-Ca²⁺-adrenergic signaling axis hyperpolarizing brown adipocytes to dampen thermogenesis and maintain tissue homeostasis. This finding reveals an electrophysiological regulatory mechanism of adipocyte function. In line with this crucial observation, we have found that the RMP of adipocytes was metabolically influenced by body weight in both humans and mice (data not shown), suggesting a vital role of adipocyte RMP in adipose tissue function. Considering the regulatory effects of Cav3.2 on RMP, we hypothesize that Cav3.2 expressed by BAT adipocytes plays an essential role in the regulation of energy expenditure. Currently, our laboratory is testing this hypothesis by selectively deleting Cav3.2 from UCP1-positive BAT adipocytes.

The energy expenditure inhibitory phenotype has been previously observed in a Vgat^{ARH} chronic inhibition mouse model, which was generated by overexpression of an inward rectifying potassium channel, Kir2.1, selectively in the Vgat^{ARH} neurons (Kir2.1OE-Vgat^{ARH}) [16]. This discrepancy suggests an ion channel-dependent inhibition on energy expenditure, which may be attributed to different levels of hyperpolarization in these two models. Although both Cav3.2KO-Vgat^{ARH} and Kir2.1OE-Vgat^{ARH} decreased spontaneous AP firing and RMP, Kir2.1OE-Vgat^{ARH} showed much higher inhibitory effects compared to Cav3.2KO-Vgat^{ARH} (Kir2.1OE-Vgat^{ARH}: -50.6 mV → -70.5 mV in RMP; Cav3.2KO-Vgat^{ARH}: -52.7 mV → -58.2 mV in RMP). The same phenotype on feeding was observed in both global Cav3.2KO mice and Cav3.2KO-Vgat^{ARH} mice, despite the wide distribution of Cav3.2s in the brain. According to the distribution data from the published Cav3.2 EGFP knock-in mice, Cav3.2 is highly expressed in the hippocampus, cortex, amygdala, hypothalamus, cerebellum, and hindbrain [82]. Our data showed that the loss of Cav3.2 in Vgat^{ARH} neurons reduced the firing activity in Vgat^{ARH} neurons, which we believe potentially contributes to the feeding behavior changes in both global and Vgat^{ARH} neuron-specific Cav3.2 KO mice. However, our data do not exclude the potential regulatory effects of Cav3.2 expressed by other brain regions on food intake. It has been shown by many human and animal studies that hippocampus [88], cortex [89], amygdala [90—

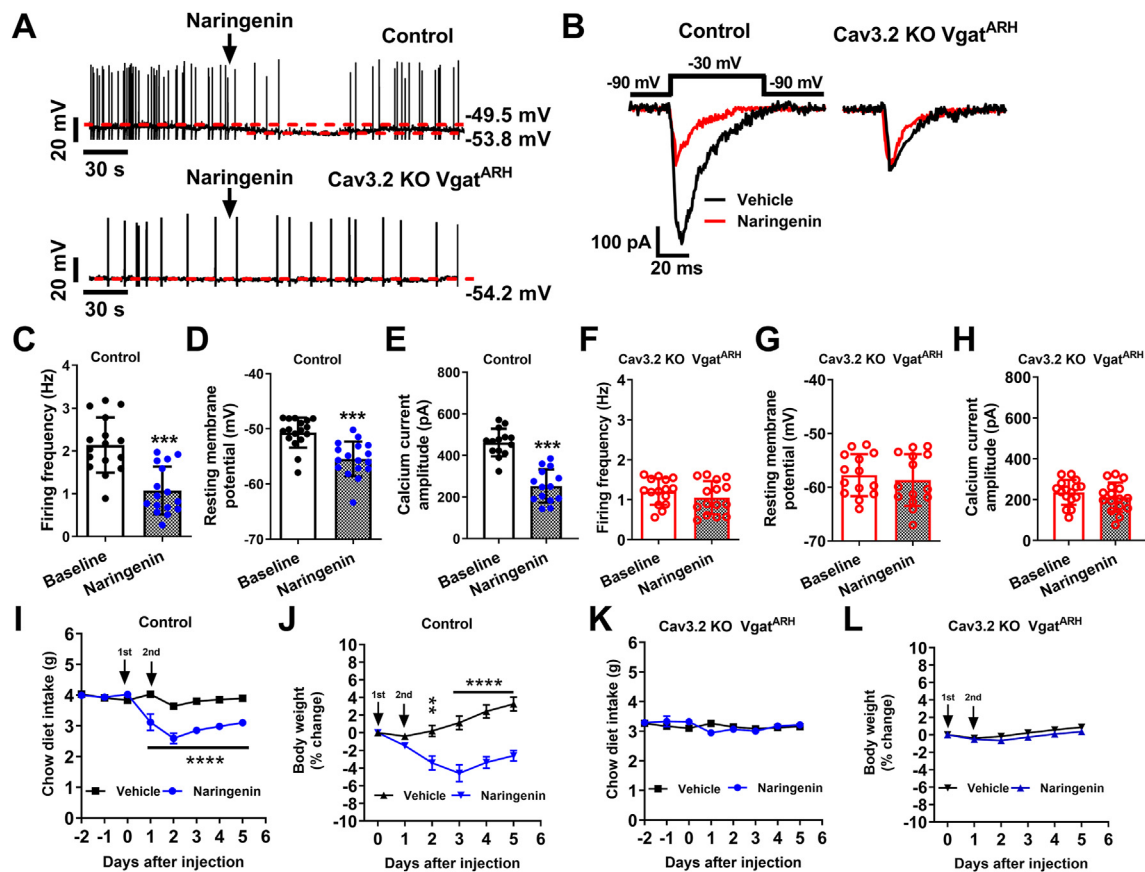


Figure 6: (See also Fig. S4). Naringenin extract reduces food intake and body weight via Cav3.2 in Vgat^{ARH} neurons. (A) Representative spontaneous action potential firing traces and (B) calcium current trace after puff naringenin treatment (40μM, 1s puff) from control and Cav3.2KO Vgat^{ARH} neurons. (C) Summary of action potential firing frequency, (D) resting membrane potential, and (E) calcium current amplitude from control Vgat^{ARH} neurons in the absence or presence of naringenin. (F) Summary of action potential firing frequency, (G) resting membrane potential, and (H) calcium current amplitude from Cav3.2KO Vgat^{ARH} neurons in the absence or presence of naringenin. (n = 14–17 neurons in each group). (I) Chow diet food intake and (J) body weight change after two doses of Naringenin or saline injection. (K) HFD food intake and (L) body weight change after two doses of Naringenin or saline injection. Results are presented as mean ± SEM. **, P < 0.01, ***, P < 0.001, ****, P < 0.0001 in two-way ANOVA analysis followed by post hoc Sidak tests.

92], cerebellum [93], and hindbrain [94,95] are all involved in regulating food intake. Cav3.2 expressed by these brain regions may contribute to different aspects of appetite control. These aspects may include declarative memory processes evaluating when, what, and how much to eat (hippocampus), interoception of food craving and executive functioning (cortex), integration of hunger, satiation, and thirst (cerebellum), sensing of peripheral hormone or nutrient fluctuation (hindbrain), and stimulation of stress-related eating (amygdala). Cav3.2 in different brain regions could regulate food intake via multiple interconnected pathways, many of which are unstudied and understudied.

Naringenin, a flavonoid belonging to the flavanones subclass, is widely distributed in various herbs and fruits, including grapefruit, citrus fruits, bergamot, tomatoes, cocoa, Greek oregano, water mint, as well as in beans [96]. Dietary naringenin supplementation within a dose range of 150–900 mg is safe in healthy adults according to a recent clinical study [40]. Ingestion of 300 mg naringenin three times/day was found to increase insulin sensitivity and decrease body weight in a recent human case study [27], suggesting naringenin as a promising therapeutic agent. However, the underlying mechanism in which naringenin modulates energy homeostasis is largely unknown. Recently, naringenin has been found to enter blood–brain barrier (BBB) [97] and

acts as a potential blocker for VGCCs, including Cav3.2 [41–43], indicating a possible central mechanism through Cav3.2. In our *ex vivo* brain slice recording study, we found that naringenin decreases the firing activity of Vgat^{ARH} neurons by inhibiting Cav3.2-mediated calcium currents. In line with these *ex vivo* observations, the inhibitory effects of naringenin on food intake and body weight were largely attenuated in Cav3.2KO mice, suggesting a Cav3.2-dependent mechanism. Our data support a model that naringenin blocks the Cav3.2 channel expressed by ARH GABAergic neurons to reduce food intake and body weight. These results also strongly argue the therapeutic potential to target Cav3.2 expressed by Vgat^{ARH} neurons in the treatment of obesity.

A majority of the rodent studies showed that 12 weeks of naringenin supplementation reduces body weight, increases insulin sensitivity, and improves lipid metabolism without affecting food intake in the obese models [98–100]. This is inconsistent with our observations that naringenin decreases food intake via Cav3.2 expressed by Vgat^{ARH} neurons. This discrepancy may be attributed to different ways of treatment or mouse models: oral supplementation vs. intraperitoneal injection; genetically obese mice vs. wild-type mice. It would also be essential to administer naringenin for a more extended period and determine whether it can induce malaise or conditioned taste aversion.

5. CONCLUSIONS

In conclusion, we found a new role of the Cav3.2 ion channel expressed by Vgat^{ARH} neurons in feeding control. In addition to the anorexic actions in animals fed ad libitum, Cav3.2 is also expected to maintain normal energy expenditure. We further provided evidence that the BBB permeable naringenin produces hypophagia-induced body weight loss by inhibiting Vgat^{ARH} neurons via Cav3.2 blockage. These results extend our understanding of Cav3.2's effects on the regulation of feeding behavior and body weight, suggesting Cav3.2 as a promising target for treating obesity and diabetes.

AUTHOR CONTRIBUTIONS

B. F. is the main contributor to the conduct of the study and data collection; J.H., N. P., H.Y., P.L., V.I., J.V., A. C., and C.R., contributed to the conduct of the study; S. Y, J.F., F.G., H.B., H. M., and C. M. contributed to the manuscript writing and data interpretation; P. X. and Y. H. contributed to the study design, data interpretation, and manuscript writing.

ACKNOWLEDGMENTS

This work was supported by grants from NIH (R01 DK123098 to P. X.; P20 GM135002 to Y. H.), DOD (Innovative Grant W81XWH-19-PRMRP-DA to P. X.), DRTC (The Pilot and Feasibility Award DK020595 to P. X.), and NIA (5K99AG065419-02 to C.J.R.). The authors wish to thank the Laboratory of Animal Center of Pennington Biomedical Research Center at Louisiana State University, and The University of Illinois at Chicago for invaluable help in mouse colony maintenance.

CONFLICT OF INTEREST

The authors declare no competing interests.

APPENDIX A. SUPPLEMENTARY DATA

Supplementary data to this article can be found online at <https://doi.org/10.1016/j.molmet.2021.101391>.

REFERENCES

- [1] Lee, J.H., Daud, A.N., Cribbs, L.L., Lacerda, A.E., Pereverzev, A., Klockner, U., et al., 1999. Cloning and expression of a novel member of the low voltage-activated T-type calcium channel family. *Journal of Neuroscience* 19(6):1912–1921.
- [2] Cribbs, L.L., Gomora, J.C., Daud, A.N., Lee, J.H., Perez-Reyes, E., 2000. Molecular cloning and functional expression of Ca(v)3.1c, a T-type calcium channel from human brain. *FEBS Letters* 466(1):54–58.
- [3] Zhuang, H., Bhattacharjee, A., Hu, F., Zhang, M., Goswami, T., Wang, L., et al., 2000. Cloning of a T-type Ca²⁺ channel isoform in insulin-secreting cells. *Diabetes* 49(1):59–64.
- [4] Gomora, J.C., Murbartian, J., Arias, J.M., Lee, J.H., Perez-Reyes, E., 2002. Cloning and expression of the human T-type channel Ca(v)3.3: insights into prepulse facilitation. *Biophysical Journal* 83(1):229–241.
- [5] Papazoglou, A., Henseler, C., Lundt, A., Wormuth, C., Soos, J., Broich, K., et al., 2017. Gender specific hippocampal whole genome transcriptome data from mice lacking the Cav2.3 R-type or Cav3.2 T-type voltage-gated calcium channel. *Data Brief* 12:81–86.
- [6] Ma, X., Zhang, Y., Zhou, H., Liu, J., Guo, F., Luo, J., et al., 2020. Silencing T-type voltage-gated calcium channel gene reduces the sensitivity of *Tetranychus cinnabarinus* (Boisduval) to scopoletin. *Comparative Biochemistry and Physiology - Part C: Toxicology & Pharmacology* 227:108644.
- [7] Talley, E.M., Cribbs, L.L., Lee, J.H., Daud, A., Perez-Reyes, E., Bayliss, D.A., 1999. Differential distribution of three members of a gene family encoding low voltage-activated (T-type) calcium channels. *Journal of Neuroscience* 19(6):1895–1911.
- [8] Jeong, K., Lee, S., Seo, H., Oh, Y., Jang, D., Choe, J., et al., 2015. Ca α 1T, a fly T-type Ca²⁺ channel, negatively modulates sleep. *Scientific Reports* 5:17893.
- [9] Pellegrini, C., Lecci, S., Luthi, A., Astori, S., 2016. Suppression of sleep spindle rhythmogenesis in mice with deletion of Cav3.2 and Cav3.3 T-type Ca(2+) channels. *Sleep* 39(4):875–885.
- [10] Gadotti, V.M., Kreitinger, J.M., Wageling, N.B., Budke, D., Diaz, P., Zamponi, G.W., 2020. Cav3.2 T-type calcium channels control acute itch in mice. *Molecular Brain* 13(1):119.
- [11] Cai, S., Gomez, K., Moutal, A., Khanna, R., 2021. Targeting T-type/Cav3.2 channels for chronic pain. *Translational Research* 234:20–30.
- [12] An, J.J., Liao, G.Y., Kinney, C.E., Sahibzada, N., Xu, B., 2015. Discrete BDNF neurons in the paraventricular hypothalamus control feeding and energy expenditure. *Cell Metabolism* 22(1):175–188.
- [13] Liu, T., Kong, D., Shah, B.P., Ye, C., Koda, S., Saunders, A., et al., 2012. Fasting activation of AgRP neurons requires NMDA receptors and involves spinogenesis and increased excitatory tone. *Neuron* 73(3):511–522.
- [14] Krashes, M.J., Shah, B.P., Koda, S., Lowell, B.B., 2013. Rapid versus delayed stimulation of feeding by the endogenously released AgRP neuron mediators GABA, NPY, and AgRP. *Cell Metabolism* 18(4):588–595.
- [15] He, Y., Shu, G., Yang, Y., Xu, P., Xia, Y., Wang, C., et al., 2016. A small potassium current in AgRP/NPY neurons regulates feeding behavior and energy metabolism. *Cell Reports* 17(7):1807–1818.
- [16] Zhu, C., Jiang, Z., Xu, Y., Cai, Z.L., Jiang, Q., Xu, Y., et al., 2020. Profound and redundant functions of arcuate neurons in obesity development. *Nat Metab* 2(8):763–774.
- [17] Xu, Y., O'Brien 3rd, W.G., Lee, C.C., Myers Jr., M.G., Tong, Q., 2012. Role of GABA release from leptin receptor-expressing neurons in body weight regulation. *Endocrinology* 153(5):2223–2233.
- [18] Wu, Q., Palmiter, R.D., 2011. GABAergic signaling by AgRP neurons prevents anorexia via a melanocortin-independent mechanism. *European Journal of Pharmacology* 660(1):21–27.
- [19] Ardianto, C., Yonemochi, N., Yamamoto, S., Yang, L., Takenoya, F., Shioda, S., et al., 2016. Opioid systems in the lateral hypothalamus regulate feeding behavior through orexin and GABA neurons. *Neuroscience* 320:183–193.
- [20] Gangarossa, G., Laffray, S., Bourinet, E., Valjent, E., 2014. T-type calcium channel Cav3.2 deficient mice show elevated anxiety, impaired memory and reduced sensitivity to psychostimulants. *Frontiers in Behavioral Neuroscience* 8:92.
- [21] Becker, A.J., Pitsch, J., Sochiwko, D., Opitz, T., Staniek, M., Chen, C.C., et al., 2008. Transcriptional upregulation of Cav3.2 mediates epileptogenesis in the pilocarpine model of epilepsy. *Journal of Neuroscience* 28(49):13341–13353.
- [22] Powell, K.L., Cain, S.M., Ng, C., Sirdesai, S., David, L.S., Kyi, M., et al., 2009. A Cav3.2 T-type calcium channel point mutation has splice-variant-specific effects on function and segregates with seizure expression in a polygenic rat model of absence epilepsy. *Journal of Neuroscience* 29(2):371–380.
- [23] Souza, I.A., Gandini, M.A., Zhang, F.X., Mitchell, W.G., Matsumoto, J., Lerner, J., et al., 2019. Pathogenic Cav3.2 channel mutation in a child with primary generalized epilepsy. *Molecular Brain* 12(1):86.
- [24] Duerschmid, C., He, Y., Wang, C., Li, C., Bournat, J.C., Romere, C., et al., 2017. Asprosin is a centrally acting orexigenic hormone. *Nature Medicine* 23(12):1444–1453.

- [25] He, Y., Xu, P., Wang, C., Xia, Y., Yu, M., Yang, Y., et al., 2020. Estrogen receptor-alpha expressing neurons in the ventrolateral VMH regulate glucose balance. *Nature Communications* 11(1):2165.
- [26] Hu, C., Rusin, C.G., Tan, Z., Guagliardo, N.A., Barrett, P.Q., 2012. Zona glomerulosa cells of the mouse adrenal cortex are intrinsic electrical oscillators. *Journal of Clinical Investigation* 122(6):2046–2053.
- [27] Murugesan, N., Woodard, K., Ramaraju, R., Greenway, F.L., Coulter, A.A., Rebello, C.J., 2020. Naringenin increases insulin sensitivity and metabolic rate: a case study. *Journal of Medicinal Food* 23(3):343–348.
- [28] Tong, Q., Ye, C.P., Jones, J.E., Elmquist, J.K., Lowell, B.B., 2008. Synaptic release of GABA by AgRP neurons is required for normal regulation of energy balance. *Nature Neuroscience* 11(9):998–1000.
- [29] Kim, E.R., Wu, Z., Sun, H., Xu, Y., Mangieri, L.R., Xu, Y., et al., 2015. Hypothalamic non-AgRP, non-POMC GABAergic neurons are required for postweaning feeding and NPY hyperphagia. *Journal of Neuroscience* 35(29):10440–10450.
- [30] Marino, R.A.M., McDevitt, R.A., Gantz, S.C., Shen, H., Pignatelli, M., Xin, W., et al., 2020. Control of food approach and eating by a GABAergic projection from lateral hypothalamus to dorsal pons. *Proceedings of the National Academy of Sciences of the United States of America* 117(15):8611–8615.
- [31] Jennings, J.H., Ung, R.L., Resendez, S.L., Stamatakis, A.M., Taylor, J.G., Huang, J., et al., 2015. Visualizing hypothalamic network dynamics for appetitive and consummatory behaviors. *Cell* 160(3):516–527.
- [32] Luo, S.X., Huang, J., Li, Q., Mohammad, H., Lee, C.Y., Krishna, K., et al., 2018. Regulation of feeding by somatostatin neurons in the tuberal nucleus. *Science* 361(6397):76–81.
- [33] Mohammad, H., Senol, E., Graf, M., Lee, C.Y., Li, Q., Liu, Q., et al., 2021. A neural circuit for excessive feeding driven by environmental context in mice. *Nature Neuroscience* 24(8):1132–1141.
- [34] Zhang, X., van den Pol, A.N., 2017. Rapid binge-like eating and body weight gain driven by zona incerta GABA neuron activation. *Science* 356(6340):853–859.
- [35] Zhao, Z.D., Chen, Z., Xiang, X., Hu, M., Xie, H., Jia, X., et al., 2019. Zona incerta GABAergic neurons integrate prey-related sensory signals and induce an appetitive drive to promote hunting. *Nature Neuroscience* 22(6):921–932.
- [36] Jacus, M.O., Uebele, V.N., Renger, J.J., Todorovic, S.M., 2012. Presynaptic Cav3.2 channels regulate excitatory neurotransmission in nociceptive dorsal horn neurons. *Journal of Neuroscience* 32(27):9374–9382.
- [37] Martinez-Hernandez, E., Zeglin, A., Almazan, E., Perissinotti, P., He, Y., Koob, M., et al., 2019. KLHL1 controls Cav3.2 expression in DRG neurons and mechanical sensitivity to pain. *Frontiers in Molecular Neuroscience* 12:315.
- [38] Cho, K.W., Kim, Y.O., Andrade, J.E., Burgess, J.R., Kim, Y.C., 2011. Dietary naringenin increases hepatic peroxisome proliferators-activated receptor alpha protein expression and decreases plasma triglyceride and adiposity in rats. *European Journal of Nutrition* 50(2):81–88.
- [39] Ke, J.Y., Kliewer, K.L., Hamad, E.M., Cole, R.M., Powell, K.A., Andridge, R.R., et al., 2015. The flavonoid, naringenin, decreases adipose tissue mass and attenuates ovarioectomy-associated metabolic disturbances in mice. *Nutrition and Metabolism* 12:1.
- [40] Rebello, C.J., Beyl, R.A., Lertora, J.J.L., Greenway, F.L., Ravussin, E., Ribnicky, D.M., et al., 2020. Safety and pharmacokinetics of naringenin: a randomized, controlled, single-ascending-dose clinical trial. *Diabetes, Obesity and Metabolism* 22(1):91–98.
- [41] Sekiguchi, F., Fujita, T., Deguchi, T., Yamaoka, S., Tomochika, K., Tsubota, M., et al., 2018. Blockade of T-type calcium channels by 6-prenylnaringenin, a hop component, alleviates neuropathic and visceral pain in mice. *Neuropharmacology* 138:232–244.
- [42] Saponara, S., Carosati, E., Mugnai, P., Sgaragli, G., Fusi, F., 2011. The flavonoid scaffold as a template for the design of modulators of the vascular Ca(v) 1.2 channels. *British Journal of Pharmacology* 164(6):1684–1697.
- [43] Zhou, Y., Cai, S., Moutal, A., Yu, J., Gomez, K., Madura, C.L., et al., 2019. The natural flavonoid naringenin elicits analgesia through inhibition of Nav1.8 voltage-gated sodium channels. *ACS Chemical Neuroscience* 10(12):4834–4846.
- [44] Yang, Z.H., Yu, H.J., Pan, A., Du, J.Y., Ruan, Y.C., Ko, W.H., et al., 2008. Cellular mechanisms underlying the laxative effect of flavonol naringenin on rat constipation model. *PLoS One* 3(10):e3348.
- [45] Pemberton, K.E., Hill-Eubanks, L.J., Jones, S.V., 2000. Modulation of low-threshold T-type calcium channels by the five muscarinic receptor subtypes in NIH 3T3 cells. *Pflügers Archiv* 440(3):452–461.
- [46] Lenglet, S., Louiset, E., Delarue, C., Vaudry, H., Contesse, V., 2002. Activation of 5-HT(7) receptor in rat glomerulosa cells is associated with an increase in adenylyl cyclase activity and calcium influx through T-type calcium channels. *Endocrinology* 143(5):1748–1760.
- [47] Kim, J.A., Park, J.Y., Kang, H.W., Huh, S.U., Jeong, S.W., Lee, J.H., 2006. Augmentation of Cav3.2 T-type calcium channel activity by cAMP-dependent protein kinase A. *Journal of Pharmacology and Experimental Therapeutics* 318(1):230–237.
- [48] Youdim, K.A., Qaiser, M.Z., Begley, D.J., Rice-Evans, C.A., Abbott, N.J., 2004. Flavonoid permeability across an in situ model of the blood-brain barrier. *Free Radical Biology and Medicine* 36(5):592–604.
- [49] Beurrier, C., Congar, P., Bioulac, B., Hammond, C., 1999. Subthalamic nucleus neurons switch from single-spike activity to burst-firing mode. *Journal of Neuroscience* 19(2):599–609.
- [50] Park, Y.G., Park, H.Y., Lee, C.J., Choi, S., Jo, S., Choi, H., et al., 2010. Ca(V) 3.1 is a tremor rhythm pacemaker in the inferior olive. *Proceedings of the National Academy of Sciences of the United States of America* 107(23):10731–10736.
- [51] Tai, C.H., Yang, Y.C., Pan, M.K., Huang, C.S., Kuo, C.C., 2011. Modulation of subthalamic T-type Ca(2+) channels remedies locomotor deficits in a rat model of Parkinson disease. *Journal of Clinical Investigation* 121(8):3289–3305.
- [52] Hahn, T.M., Breininger, J.F., Baskin, D.G., Schwartz, M.W., 1998. Coexpression of AgRP and NPY in fasting-activated hypothalamic neurons. *Nature Neuroscience* 1(4):271–272.
- [53] Chen, Y., Essner, R.A., Kosar, S., Miller, O.H., Lin, Y.C., Mesgarzadeh, S., et al., 2019. Sustained NPY signaling enables AgRP neurons to drive feeding. *Elife* 8.
- [54] Chen, Y., Lin, Y.C., Zimmerman, C.A., Essner, R.A., Knight, Z.A., 2016. Hunger neurons drive feeding through a sustained, positive reinforcement signal. *Elife* 5.
- [55] Dubois, C.J., Ramamoorthy, P., Whim, M.D., Liu, S.J., 2012. Activation of NPY type 5 receptors induces a long-lasting increase in spontaneous GABA release from cerebellar inhibitory interneurons. *Journal of Neurophysiology* 107(6):1655–1665.
- [56] Nakajima, K., Cui, Z., Li, C., Meister, J., Cui, Y., Fu, O., et al., 2016. Gs-coupled GPCR signalling in AgRP neurons triggers sustained increase in food intake. *Nature Communications* 7:10268.
- [57] Aponte, Y., Atasoy, D., Sternson, S.M., 2011. AGRP neurons are sufficient to orchestrate feeding behavior rapidly and without training. *Nature Neuroscience* 14(3):351–355.
- [58] Atasoy, D., Betley, J.N., Su, H.H., Sternson, S.M., 2012. Deconstruction of a neural circuit for hunger. *Nature* 488(7410):172–177.
- [59] Krashes, M.J., Shah, B.P., Madara, J.C., Olson, D.P., Strohlic, D.E., Garfield, A.S., et al., 2014. An excitatory paraventricular nucleus to AgRP neuron circuit that drives hunger. *Nature* 507(7491):238–242.
- [60] Lee, S.Y., Masaoka, T., Han, H.S., Matsuzaki, J., Hong, M.J., Fukuhara, S., et al., 2016. A prospective study on symptom generation according to spicy food intake and TRPV1 genotypes in functional dyspepsia patients. *Neuro-Gastroenterology and Motility* 28(9):1401–1408.

- [61] Jeong, J.H., Lee, D.K., Liu, S.M., Chua Jr., S.C., Schwartz, G.J., Jo, Y.H., 2018. Activation of temperature-sensitive TRPV1-like receptors in ARC POMC neurons reduces food intake. *PLoS Biology* 16(4):e2004399.
- [62] Del Prete, E., Lutz, T.A., Scharer, E., 1996. Inhibition of food intake in rats by the K⁺ channel opener cromakalim. *Pharmacology Biochemistry and Behavior* 53(4):839–842.
- [63] Zhang, Z., Zhang, W., Jung, D.Y., Ko, H.J., Lee, Y., Friedline, R.H., et al., 2012. TRPM2 Ca²⁺ channel regulates energy balance and glucose metabolism. *American Journal of Physiology. Endocrinology and Metabolism* 302(7):E807–E816.
- [64] Soares, M.J., Pathak, K., Calton, E.K., 2014. Calcium and vitamin D in the regulation of energy balance: where do we stand? *International Journal of Molecular Sciences* 15(3):4938–4945.
- [65] Valdecabres, A., Pires, J.A.A., Silva-Del-Rio, N., 2018. Effect of prophylactic oral calcium supplementation on postpartum mineral status and markers of energy balance of multiparous Jersey cows. *Journal of Dairy Science* 101(5):4460–4472.
- [66] Lussier, B.T., Moor, B.C., French, M.B., Kraicer, J., 1988. Release of growth hormone from purified somatotrophs: effects of the calcium channel antagonists diltiazem and nifedipine on release induced by growth hormone-releasing factor. *Canadian Journal of Physiology and Pharmacology* 66(11):1373–1380.
- [67] Watanabe, M., Sakuma, Y., Kato, M., 2004. High expression of the R-type voltage-gated Ca²⁺ channel and its involvement in Ca²⁺-dependent gonadotropin-releasing hormone release in GT1-7 cells. *Endocrinology* 145(5):2375–2383.
- [68] Li, Y.B., Pei, X.Y., Wang, D., Chen, C.H., Cai, M.J., Wang, J.X., et al., 2017. The steroid hormone 20-hydroxyecdysone upregulates calcium release-activated calcium channel modulator 1 expression to induce apoptosis in the midgut of *Helicoverpa armigera*. *Cell Calcium* 68:24–33.
- [69] Pershadsingh, H.A., Gale, R.D., Delfert, D.M., McDonald, J.M., 1986. A calmodulin dependent Ca²⁺-activated K⁺ channel in the adipocyte plasma membrane. *Biochemical and Biophysical Research Communications* 135(3):934–941.
- [70] Prudente, S., Flex, E., Morini, E., Turchi, F., Capponi, D., De Cosmo, S., et al., 2007. A functional variant of the adipocyte glycerol channel aquaporin 7 gene is associated with obesity and related metabolic abnormalities. *Diabetes* 56(5):1468–1474.
- [71] Li, F.N., Yin, J.D., Ni, J.J., Liu, L., Zhang, H.Y., Du, M., 2010. Chloride intracellular channel 5 modulates adipocyte accumulation in skeletal muscle by inhibiting preadipocyte differentiation. *Journal of Cellular Biochemistry* 110(4):1013–1021.
- [72] Nishizuka, M., Hayashi, T., Asano, M., Osada, S., Imagawa, M., 2014. KCNK10, a tandem pore domain potassium channel, is a regulator of mitotic clonal expansion during the early stage of adipocyte differentiation. *International Journal of Molecular Sciences* 15(12):22743–22756.
- [73] Zemel, M.B., Kim, J.H., Woychik, R.P., Michaud, E.J., Kadwell, S.H., Patel, I.R., et al., 1995. Agouti regulation of intracellular calcium: role in the insulin resistance of viable yellow mice. *Proceedings of the National Academy of Sciences of the United States of America* 92(11):4733–4737.
- [74] Lein, E.S., Hawrylycz, M.J., Ao, N., Ayres, M., Bensinger, A., Bernard, A., et al., 2007. Genome-wide atlas of gene expression in the adult mouse brain. *Nature* 445(7124):168–176.
- [75] Nahm, S.S., Farnell, Y.Z., Griffith, W., Earnest, D.J., 2005. Circadian regulation and function of voltage-dependent calcium channels in the suprachiasmatic nucleus. *Journal of Neuroscience* 25(40):9304–9308.
- [76] McNally, B.A., Plante, A.E., Meredith, A.L., 2020. Diurnal properties of voltage-gated Ca(2+) currents in suprachiasmatic nucleus and roles in action potential firing. *Journal of Physiology* 598(9):1775–1790.
- [77] Buijs, F.N., Guzman-Ruiz, M., Leon-Mercado, L., Basualdo, M.C., Escobar, C., Kalsbeek, A., et al., 2017. Suprachiasmatic nucleus interaction with the arcuate nucleus; essential for organizing physiological rhythms. *eNeuro* 4(2).
- [78] Mendez-Hernandez, R., Escobar, C., Buijs, R.M., 2020. Suprachiasmatic nucleus-arcuate nucleus Axis: interaction between time and metabolism essential for health. *Obesity* 28(Suppl 1):S10–S17.
- [79] Chen, Y., Zeng, X., Huang, X., Serag, S., Woolf, C.J., Spiegelman, B.M., 2017. Crosstalk between KCNK3-mediated ion current and adrenergic signaling regulates adipose thermogenesis and obesity. *Cell* 171(4):836–848 e813.
- [80] Li, S., Hao, M., Li, B., Chen, M., Chen, J., Tang, J., et al., 2020. CACNA1H downregulation induces skeletal muscle atrophy involving endoplasmic reticulum stress activation and autophagy flux blockade. *Cell Death & Disease* 11(4):279.
- [81] Zholos, A.V., Fenech, C.J., Prestwich, S.A., Bolton, T.B., 2000. Membrane currents in cultured human intestinal smooth muscle cells. *Journal of Physiology* 528(Pt 3):521–537.
- [82] Bernal Sierra, Y.A., Haseleu, J., Kozlenkov, A., Begay, V., Lewin, G.R., 2017. Genetic tracing of Cav3.2 T-type calcium channel expression in the peripheral nervous system. *Frontiers in Molecular Neuroscience* 10:70.
- [83] Watanabe, M., Ueda, T., Shibata, Y., Kumamoto, N., Shimada, S., Ugawa, S., 2015. Expression and regulation of Cav3.2 T-type calcium channels during inflammatory hyperalgesia in mouse dorsal root ganglion neurons. *PLoS One* 10(5):e0127572.
- [84] Cai, S., Gomez, K., Moutal, A., Khanna, R., 2021. Targeting T-type/Cav3.2 channels for chronic pain. *Translational Research* 234:20–30.
- [85] Harraz, O.F., Abd El-Rahman, R.R., Bigdely-Shamloo, K., Wilson, S.M., Brett, S.E., Romero, M., et al., 2014. Ca(V)3.2 channels and the induction of negative feedback in cerebral arteries. *Circulation Research* 115(7):650–661.
- [86] Harraz, O.F., Brett, S.E., Zechariah, A., Romero, M., Puglisi, J.L., Wilson, S.M., et al., 2015. Genetic ablation of Cav3.2 channels enhances the arterial myogenic response by modulating the RyR-BKCa axis. *Arteriosclerosis, Thrombosis, and Vascular Biology* 35(8):1843–1851.
- [87] Abdul Kadir, L., Stacey, M., Barrett-Jolley, R., 2018. Emerging roles of the membrane potential: action beyond the action potential. *Frontiers in Physiology* 9:1661.
- [88] Stevenson, R.J., Francis, H.M., 2017. The hippocampus and the regulation of human food intake. *Psychological Bulletin* 143(10):1011–1032.
- [89] Gluck, M.E., Viswanath, P., Stinson, E.J., 2017. Obesity, appetite, and the prefrontal cortex. *Curr Obes Rep* 6(4):380–388.
- [90] Douglass, A.M., Kucukdereli, H., Ponserre, M., Markovic, M., Grundemann, J., Strobel, C., et al., 2017. Central amygdala circuits modulate food consumption through a positive-valence mechanism. *Nature Neuroscience* 20(10):1384–1394.
- [91] Park-York, M., Boghossian, S., Oh, H., York, D.A., 2013. PKC θ expression in the amygdala regulates insulin signaling, food intake and body weight. *Obesity* 21(4):755–764.
- [92] Areias, M.F., Prada, P.O., 2015. Mechanisms of insulin resistance in the amygdala: influences on food intake. *Behavioural Brain Research* 282:209–217.
- [93] Zhu, J.N., Wang, J.J., 2008. The cerebellum in feeding control: possible function and mechanism. *Cellular and Molecular Neurobiology* 28(4):469–478.
- [94] Huang, K.P., Raybould, H.E., 2020. Estrogen and gut satiety hormones in vagus-hindbrain axis. *Peptides* 133:170389.
- [95] Wright, J., Campos, C., Herzog, T., Covasa, M., Czaja, K., Ritter, R.C., 2011. Reduction of food intake by cholecystokinin requires activation of hindbrain NMDA-type glutamate receptors. *American Journal of Physiology - Regulatory, Integrative and Comparative Physiology* 301(2):R448–R455.
- [96] Alam, P., Parvez, M.K., Arbab, A.H., Al-Dosari, M.S., 2017. Quantitative analysis of rutin, quercetin, naringenin, and gallic acid by validated RP- and NP-HPLC methods for quality control of anti-HBV active extract of *Guiera senegalensis*. *Pharmazie Biologischer* 55(1):1317–1323.

- [97] Youdim, K.A., Dobbie, M.S., Kuhnle, G., Proteggente, A.R., Abbott, N.J., Rice-Evans, C., 2003. Interaction between flavonoids and the blood-brain barrier: in vitro studies. *Journal of Neurochemistry* 85(1):180–192.
- [98] Mulvihill, E.E., Allister, E.M., Sutherland, B.G., Telford, D.E., Sawyez, C.G., Edwards, J.Y., et al., 2009. Naringenin prevents dyslipidemia, apolipoprotein B overproduction, and hyperinsulinemia in LDL receptor-null mice with diet-induced insulin resistance. *Diabetes* 58(10): 2198–2210.
- [99] Assini, J.M., Mulvihill, E.E., Sutherland, B.G., Telford, D.E., Sawyez, C.G., Felder, S.L., et al., 2013. Naringenin prevents cholesterol-induced systemic inflammation, metabolic dysregulation, and atherosclerosis in *Ldlr*(-/-) mice. *The Journal of Lipid Research* 54(3):711–724.
- [100] Assini, J.M., Mulvihill, E.E., Burke, A.C., Sutherland, B.G., Telford, D.E., Chhoker, S.S., et al., 2015. Naringenin prevents obesity, hepatic steatosis, and glucose intolerance in male mice independent of fibroblast growth factor 21. *Endocrinology* 156(6):2087–2102.